

Effect of iron doping and oxygen stoichiometry on infrared absorption in $Y_1Ba_2Cu_3O_{7-\delta}$

A K SOOD[†], K SANKARAN*, Y HARIHARAN,
S VIJAYALAKSHMI*, V SANKARA SASTRY,
S KALAVATHI and J JANAKI

Materials Science Laboratory, *Radiochemistry Programme, Indira Gandhi Centre for Atomic Research, Kalpakkam 603 102, India

[†]Present address: Department of Physics, Indian Institute of Science, Bangalore 560 012, India

MS received 29 July 1988

Abstract. We report infrared absorption of $Y_1Ba_2Cu_3O_{7-\delta}$ as a function of oxygen stoichiometry ($0 < \delta < 1$) and copper substitution by iron in the spectral range of 450–700 cm^{-1} . The strong bands associated with Cu-O vibrations undergo significant changes in their frequencies and intensities as δ is varied across the orthorhombic to tetragonal phase. These changes coupled with those arising as a result of doping with iron has helped in identifying the nature of the vibrational modes.

Keywords. YBCO; iron-doped YBCO; oxygen stoichiometry; superconductivity; infrared absorption.

PACS Nos 78-30, 74-90, 74-70

1. Introduction

The high temperature superconductivity of $Y_1Ba_2Cu_3O_{7-\delta}$ (YBCO) is being investigated extensively by infrared and Raman spectroscopy among a number of other experimental techniques. It is expected that spectroscopic techniques will help in elucidating the nature of phonons and the role of electron-phonon interaction in the superconductivity of these systems. It is now well established that the crystal structure of YBCO is either orthorhombic or tetragonal depending on the oxygen deficiency (δ) and ordering of oxygen over the two available sites on the a and b axis. There are two distinct sites for Cu; one site labelled Cu(1) is between the two Ba-planes and forms one-dimensional Cu(1)–O(1) chains in the orthorhombic phase. The other site Cu(2) situated between the Y and Ba planes forms puckered two-dimensional Cu(2)–O(2, 3) planes (Beno *et al* 1987). As a step towards understanding the mechanism of superconductivity with particular reference to the role of Cu-O chains and layers, the effect of oxygen stoichiometry and the impurity elements substituted for Cu has been investigated. It has been recently shown that the substitution of Cu in YBCO by a number of metal atoms like Fe, Co, Ni, Ga and Al up to a certain fraction converts the orthorhombic structure to the tetragonal one without destroying the superconductivity (Maeno *et al* 1987; Takayama-Muromachi *et al* 1987 and references therein). These studies suggest that orthorhombicity is not essential, as was earlier conjectured, for the occurrence of superconductivity. It may also be added that some authors (Hiroi *et al*

1988) find evidence of orthorhombicity in iron-doped samples on a microscopic scale even though the structure is tetragonal as seen by X-ray and neutron powder diffraction.

A number of Raman (Thomsen *et al* 1988a, b and references therein) and infrared (IR) experiments (Bonn *et al* 1988 and references therein) have been carried out on YBCO, also as a function of temperature, with a broad aim to determine the symmetry and nature of the phonons and the superconducting gap. Raman and IR spectra have also been studied as a function of the oxygen stoichiometry (Saito *et al* 1987; Sugai 1987; Thomsen *et al* 1988b and Ruani *et al* 1988). The observed modes in the range 50–400 cm^{-1} have been assigned with some reliability but disagreement in the literature exists over the nature of peaks between 450 and 700 cm^{-1} , a region of Cu-O vibrations. In this paper we report the infrared absorption of YBCO as a function of iron doping and δ in order to understand the vibrational modes in the range 450–700 cm^{-1} . Although a number of Mössbauer experiments have been done on Fe doped YBCO (for example, Nasu *et al* 1987) there has been no report on the vibrational characteristics as a function of iron doping. The presence of certain modes in the iron doped samples leads us to believe that their structure is indeed tetragonal as seen in our X-ray measurements. Our results on the effect of oxygen stoichiometry are similar to those of Ruani *et al* (1988) which appeared while our work was nearing completion.

2. Experimental

Samples of $\text{Y}_1\text{Ba}_2\text{Cu}_3\text{O}_{7-\delta}$ with different δ were prepared by heating in oxygen atmosphere for one hour at different temperatures (300° to 900°C) followed by quenching in liquid nitrogen. The detailed procedures for preparation and characterization by X-ray diffraction, weight loss, a.c. susceptibility and room temperature resistivity are described by Bharathi *et al* (1988) and Hariharan *et al* (1988). The Fe-doped samples, $\text{Y}_1\text{Ba}_2(\text{Cu}_{1-x}\text{Fe}_x)_3\text{O}_{7-\delta}$ were prepared by standard solid state reaction route for $x = 0.01, 0.02, 0.05$ and 0.10 by mixing the correct amount of Fe_2O_3 with the starting materials Y_2O_3 , BaCO_3 and CuO and then subsequent heating and sintering (Bharathi *et al* 1988). The ratio of Fe/Cu determined by atomic absorption spectroscopy agreed with the above quoted values to within $\pm 10\%$. The samples were characterized by powder X-ray diffraction (using Siemens X-ray diffractometer, model D500) and a.c. susceptibility (Hariharan *et al* 1988). Figure 1 shows the X-ray diffraction pattern for all the four Fe-doped samples along with YBCO with $\delta = 0.12$ (orthorhombic and superconducting) and $\delta = 0.75$ (tetragonal and non-superconducting). The crystal structures (orthorhombic or tetragonal) were determined by a least squares fitting of all the d -spacings in the angular range 10° to $70^\circ 2\theta$ for $\text{CuK}_{\alpha 1}$ radiation. Table 1 summarizes the crystal structure and T_c onset by a.c. susceptibility for different doped samples. No impurity phases were detected in the X-ray diffraction pattern.

The infrared absorption spectra were recorded at room temperature using Digilab FTIR spectrophotometer model 15/90 by standard KBr pellet technique; the weight percentage of the sample being 2.5% (mole percentage of 0.45%). The amount of the

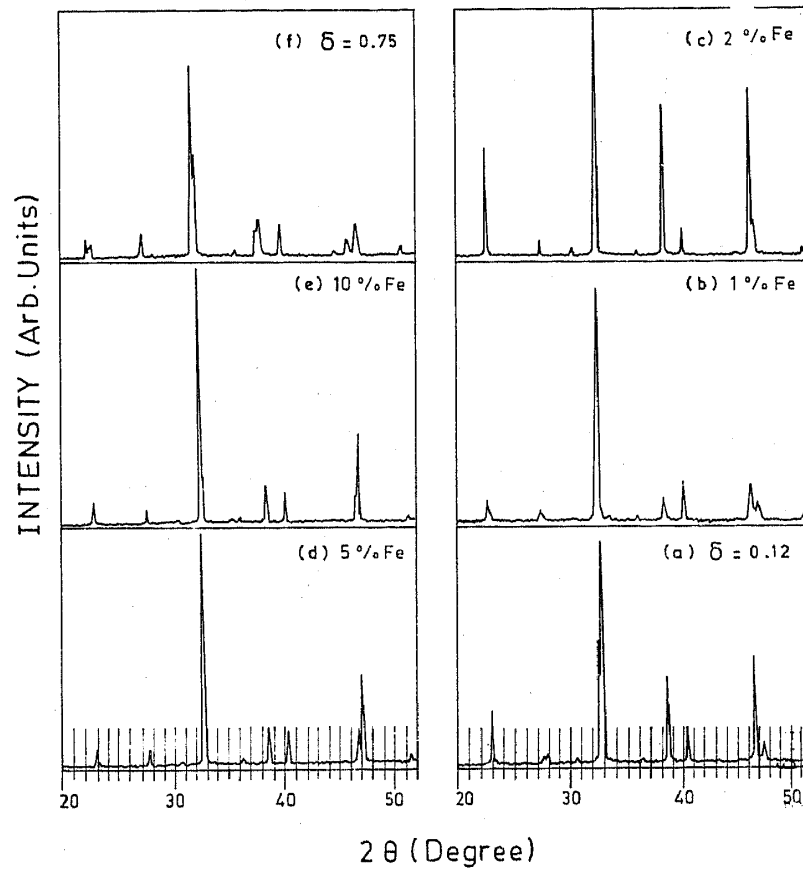


Figure 1. X-ray diffraction pattern recorded using Cu-K $_{\alpha 1}$ radiation. (a) YBCO ($\delta = 0.12$, superconducting); (b) iron doped, $x = 0.01$; (c) $x = 0.02$; (d) $x = 0.05$; (e) $x = 0.10$; (f) YBCO ($\delta = 0.75$, non-superconducting). Note the differences in doublets at $2\theta \sim 33^\circ$ and $2\theta \sim 47^\circ$

Table 1. Crystal structure, lattice parameters and T_c onset in $\text{YBa}_2(\text{Cu}_{1-x}\text{Fe}_x)_3\text{O}_{7-\delta}$

x	Structure	Lattice parameters (\AA)	T_c onset (K)
0.01	Orthorhombic	$a = 3.837$ $b = 3.882$ $c = 11.673$	90.8
0.02	Tetragonal	$a = b = 3.863$ $c = 11.675$	84.8
0.05	Tetragonal	$a = b = 3.866$ $c = 11.681$	71.0
0.10	Tetragonal	$a = b = 3.870$ $c = 11.666$	54.0

sample was kept the same (within $\pm 1\%$) for all the measurements. It may be remarked that although the detailed lineshape may somewhat depend on the sample particle size in the KBr pellet technique, the peak positions are unambiguously determined.

3. Results

3.1 Effect of oxygen stoichiometry

Figure 2(a) shows the absorption spectra of eight samples with different oxygen deficiency δ varying between 0.12 (curve 1) to 0.75 (curve 8). The sample is orthorhombic for $\delta \leq 0.52$, a mixture of orthorhombic and tetragonal phases for $\delta = 0.62$ and tetragonal for $\delta = 0.67$ and 0.75. The samples with δ equal to 0.67 and 0.75 were non-superconducting. The spectra are similar to those of Ruani *et al* (1988).

It is seen from figure 2(a) that the phonon bands are superimposed on a strong absorption background for superconducting samples, $\delta < 0.62$, and have been attributed to the onset of an electronic transition (Ruani *et al* 1988). We suggest that the

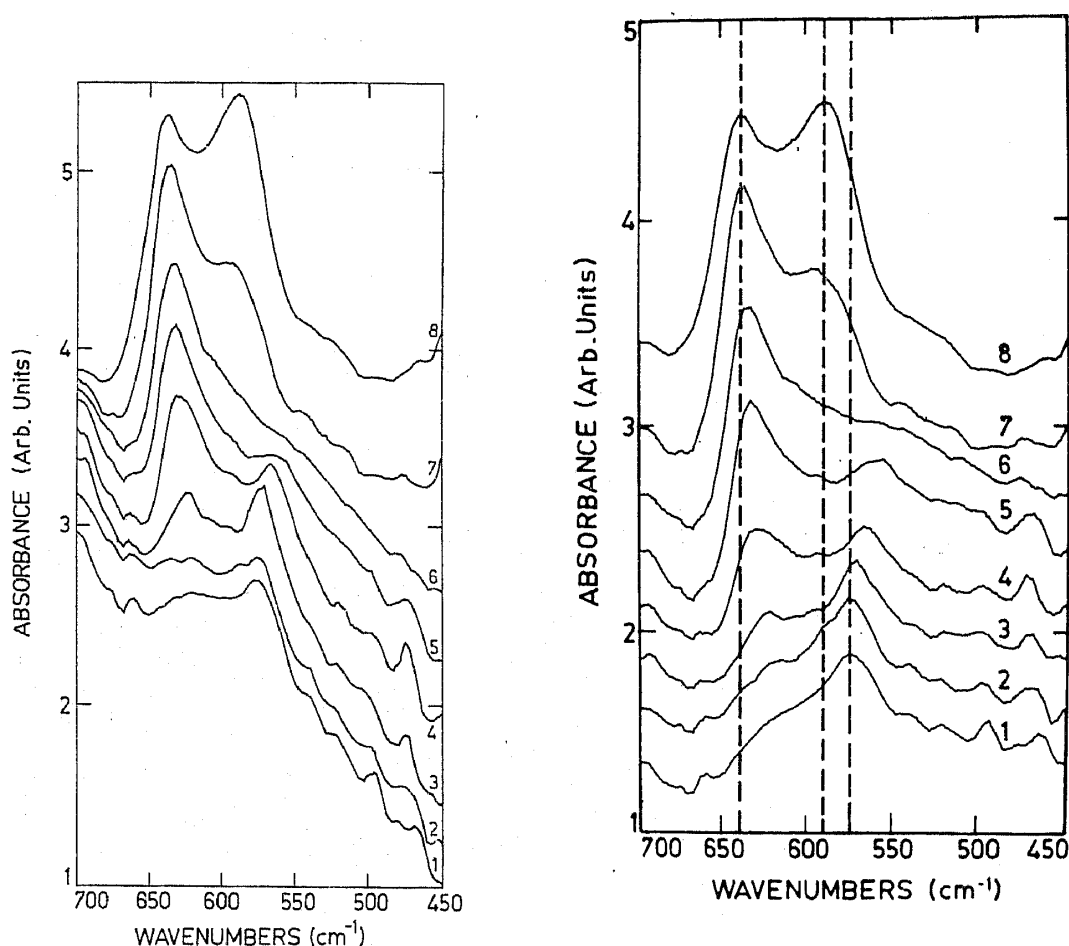


Figure 2(a). Infrared absorption spectra for $Y_1Ba_2Cu_3O_{7-\delta}$ with different oxygen stoichiometry. (1) $\delta = 0.12$; (2) $\delta = 0.17$; (3) $\delta = 0.22$; (4) $\delta = 0.43$; (5) $\delta = 0.52$; (6) $\delta = 0.62$; (7) $\delta = 0.67$; (8) $\delta = 0.75$.

Figure 2(b). Absorption spectra after subtracting the constant slope electronic absorption background. The curve numbers are same as for figure 2(a). The vertical dotted lines are drawn at 575, 590 and 640 cm^{-1} to facilitate comparison of positions of the main bands.

electronic transition can be the charge-transfer transitions involving transfer of a hole from Cu to oxygen orbitals which have been observed in optical reflectivity experiments on the superconducting YBCO at $\sim 3000\text{ cm}^{-1}$ and not seen in nonsuperconducting phase (Kamaras *et al* 1987). In order to see the phonons more clearly, the electronic absorption (with a constant slope) has been subtracted from the spectra and the results are shown in figure 2(b). The band positions are plotted as a function of δ in figure 3. The phonon energies agree with the values obtained by Sugai (1987) from the Kramer-Kronig transform of the reflectivity data and with those of absorption measurements of Saito *et al* (1987).

3.2 Effect of iron doping

Figure 4(a) shows the absorption spectra of $\text{Y}_1\text{Ba}_2(\text{Cu}_{1-x}\text{Fe}_x)_3\text{O}_{7-\delta}$ for $x = 0.01, 0.02, 0.05$ and 0.10 along with YBCO ($\delta = 0.1$ for curve 1 and $\delta = 0.75$ for curve 6) for comparison. All the spectra for different x values exhibit a strong electronic absorption background. This is consistent with the fact that all the Fe-doped YBCO are superconducting and can have charge transfer transitions. The corresponding background subtracted spectra are shown in figure 4(b).

4. Discussion

In $\text{Y}_1\text{Ba}_2\text{Cu}_3\text{O}_{6.88}$ (curve 1 in figure 2b) the main phonon absorption bands are at 575 cm^{-1} and 621 cm^{-1} . As δ increases, the 621 cm^{-1} mode shifts to higher frequencies

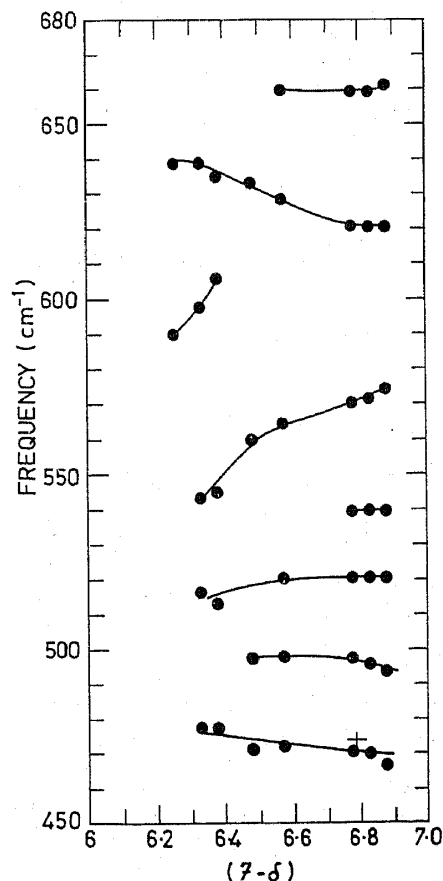


Figure 3. Observed absorption peak positions in figure 2(b) as a function of $(7 - \delta)$.

($\sim 640 \text{ cm}^{-1}$ for $\delta = 0.75$) and gains in oscillator strength. On the other hand, the 575 cm^{-1} mode shifts to lower frequencies and reduces in intensity as δ increases, so much so that it disappears in samples with $\delta > 0.62$. A strong mode appears at 590 cm^{-1} in the tetragonal phase with $\delta = 0.75$.

In iron-doped samples, the 575 cm^{-1} band is present in orthorhombic ($x = 0.01$) as well as in tetragonal phases ($x = 0.02, 0.05$ and 0.10). It can also be seen from curve 4 ($x = 0.05$) and curve 5 ($x = 0.10$) of figure 4(b) that a band centred at $\sim 590 \text{ cm}^{-1}$ is also present. The 621 cm^{-1} mode shifts to lower frequencies with increased iron doping. The intensity of the mode near 660 cm^{-1} increases with x .

4.1 Mode at 575 cm^{-1}

There have been two possible assignments made to the 575 cm^{-1} mode. Ruani *et al* (1988) suggested that the 575 cm^{-1} mode is due to the activation of a totally symmetric stretch Raman mode because of its coupling with the low energy electronic absorption arising from the charge carriers. On the other hand, Thomsen *et al* (1988) attribute this mode either to Cu(1)–O(4) stretch (A_{2u} symmetry) or Cu(2)–O(2, 3) vibrations (with polarization along x or y). We have used the notation of Beno *et al* (1987) for labelling the oxygen atoms where O(1) atoms are along chains in the basal plane and O(4) is bridging oxygen between Cu(1) and Cu(2). We associate the 575 cm^{-1} mode with Cu(1)–O(4) anti-symmetric stretch vibrations for the following reasons. The oscillator strength of the mode is expected to depend on its interaction with electronic excitations like charge-transfer excitations (Rice and Wang 1987; Jayadev *et al* 1988). The decrease in the intensity of the mode with increase in δ can be due to the reduction in charge-transfer excitations which are shown to be absent for $\delta \sim 0.8$ (Kamaras *et al* 1987). The observation of strong 575 cm^{-1} mode in iron-doped YBCO (tetragonal but superconducting) is also understandable because charge-transfer excitations will be present in these superconducting samples. As δ increases, the Cu(1)–O(4) bond length decreases even though c -axis increases (Santoro *et al* 1987). This should have resulted in the increase of the vibrational frequency. But the increase due to decreased bond length is overcompensated by the accompanying decrease in the charge state of Cu(1). This is the same reason attributed by Kourouklis *et al* (1987) to the decrease of the A_{1g} Raman mode frequency from 502 cm^{-1} ($\delta = 0$) to 480 cm^{-1} ($\delta = 1$).

4.2 Mode at 621 cm^{-1}

We assign the 621 cm^{-1} mode in sample with $\delta = 0.12$ (curve 1 in figure 2b) and iron-doped samples (figure 4b) to Cu(2)–O(2, 3) vibrations with the polarization in xy plane (symmetry B_{2u}, B_{3u} in the orthorhombic phase and E_u in the tetragonal phase). This mode is weaker than the 575 cm^{-1} in the superconducting samples (undoped or Fe-doped and becomes strong in the non-superconducting, semiconducting sample ($\delta = 0.75$; curve 8 in figure 2b). This can be understood by realizing that in the two-dimensional metals free carriers completely screen the electric field accompanying the phonons with the polarization in the xy plane (Sugai 1987). The screening is much less for phonons with the polarization along z -direction, e.g., for the 575 cm^{-1} mode (A_{2u} symmetry). Further, the screening for B_{2u}, B_{3u} phonons will decrease as the number of free carriers reduce (manifested in normal state resistivity, Hariharan *et al* 1988) with increase in δ .

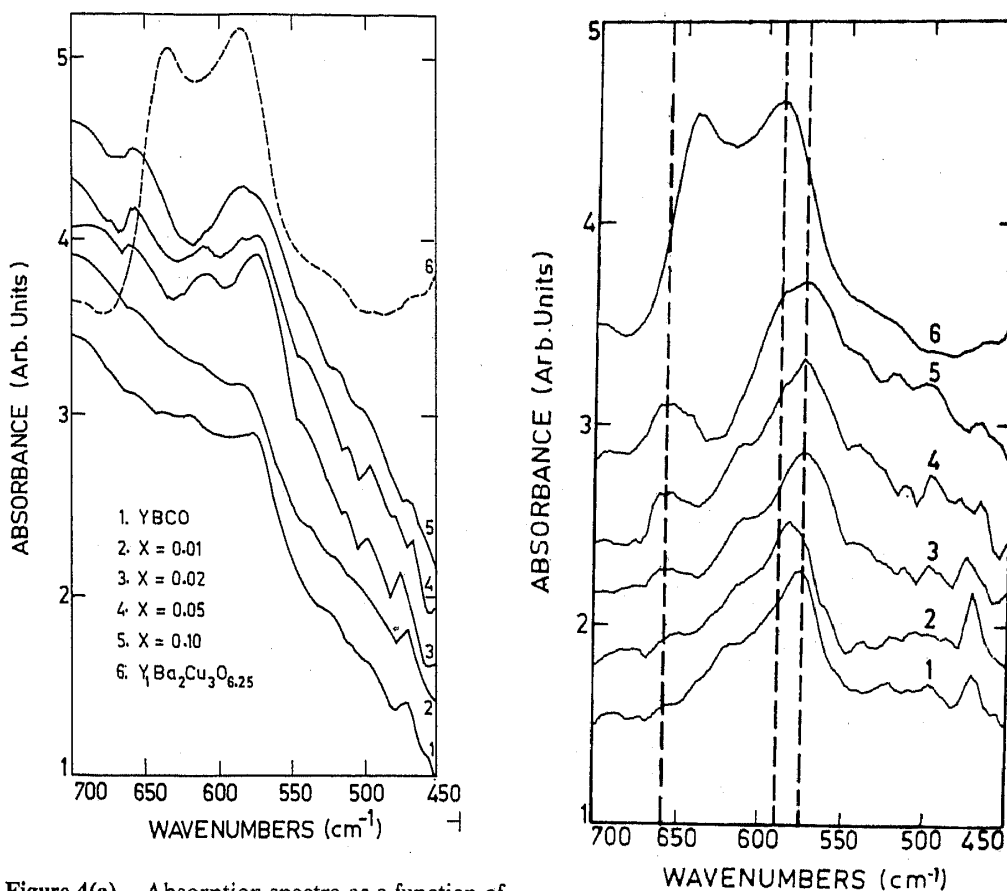


Figure 4(a). Absorption spectra as a function of iron doping x in $\text{Y}_1\text{Ba}_2(\text{Cu}_{1-x}\text{Fe}_x)_3\text{O}_{7-\delta}$. Curve (1) Undoped YBCO ($x=0$), $\delta \sim 0.1$; (2) $x=0.01$; (3) $x=0.02$; (4) $x=0.05$; (5) $x=0.10$; (6) YBCO ($x=0$); $\delta=0.75$.

Figure 4(b). Background subtracted spectra obtained from figure 4(a).

There has been considerable controversy over the assignment of a mode near $\sim 640 \text{ cm}^{-1}$ in the Raman spectra of YBCO. Although Blumenroder *et al* (1987) assign it to the Cu(1)–O(1) defect induced vibrations, most of the other workers attribute it to the impurity phase, BaCuO_2 (Kirby *et al* 1987) which has a Raman mode at $\sim 640 \text{ cm}^{-1}$. To check if this mode is IR active, we prepared BaCuO_2 (characterized by X-ray diffraction) and recorded its IR spectrum which shows absorption modes at 478, 532 and 583 cm^{-1} . This rules out the possibility of the 640 cm^{-1} mode observed in IR absorption of YBCO with $\delta=0.75$ (see curve 8 in figure 2(b)) to be assigned to the impurity phase BaCuO_2 .

4.3 Mode at 590 cm^{-1} in the nonsuperconducting samples

The fact that the strong 590 cm^{-1} band in YBCO ($\delta=0.75$) disappears as δ decreases has led to the suggestion that the mode is related to the defect vibrations localized in the vicinity of O(1) site (Ruani *et al* 1988). The 590 cm^{-1} band envelope represents the phonon density of states profile of the Cu(1)–O(1) stretching mode due to defect-induced wavevector non-conservation ($k \neq 0$) transitions. The appearance of the 590 cm^{-1} mode in the iron doped samples (curves 4 and 5 in figure 4(b)) suggests that the structure of the iron doped YBCO is indeed tetragonal as observed in the X-ray.

This can be understood from the fact that Fe favours 6-fold co-ordination (Oda *et al* 1987; Takayama-Muromachi *et al* 1987) which is reflected in the Mössbauer spectra along with 2 and 4 fold co-ordination. The two and six-fold co-ordination can come about, in a non-oxygen deficient compound, by the shifting of the oxygen atoms from the O(1) (along *b* axis) site in one unit cell to O(5) vacant sites (along *a* axis) in different unit cell. Since the orthorhombicity in YBCO is believed to arise from the ordering of the oxygen vacancies, the shifting of oxygen atoms from O(1) to O(5) sites induced by the doped iron atoms will disrupt this ordering and make the structure tetragonal. The presence of iron-induced disorder is reflected in the appearance of the 590 cm^{-1} mode in figure 4(b), in agreement with Ruani *et al* (1988).

4.4 Fe-O vibrational modes

It has been shown that Fe predominantly substitutes Cu(1) (Roth *et al* 1988 and references therein). Since the charge state of Fe is +3 compared to $\sim +2$ for Cu(1) and Fe-O(1) bond length is smaller as compared with Cu(1)-O(1) (see table 1 for the decrease in *b*-axis as *x* increases), the vibrational frequency of Fe-O(1) stretching will be larger than that of Cu(1)-O(1) stretching mode. The latter, it has been argued earlier, occurs at $\sim 590\text{ cm}^{-1}$. Figure 4(b) shows that a band centred at $\sim 660\text{ cm}^{-1}$ increases as the iron content increases, suggesting it to be related to Fe-O(1) vibrations.

5. Conclusions

Infrared absorption spectra have been studied in YBCO as a function of oxygen stoichiometry and iron doping in the range $450\text{--}700\text{ cm}^{-1}$. These studies have helped in the assignment of the infrared active Cu-O modes. IR results further point out that doping with Fe makes the structure tetragonal in conformity with the X-ray measurements.

Acknowledgements

The authors would like to thank Dr T S Radhakrishnan, Dr P Rodriguez and Dr C K Mathews for their encouragement during the course of these experiments.

References

- Beno M A, Soderholm L, Capone D W, Hinks D G, Jorgensen J D, Schuller I K, Segre C U, Zhang K and Grace J D 1987 *Appl. Phys. Lett.* **51** 57
- Bharathi A, Hariharan Y, Sood A K, Sastry V S, Janawadkar M P and Sundar C S 1988 *Europhysics Lett.* **6** 369
- Bonn D A, O'Reilly A H, Greedan J E, Stager C V, Timusk T, Kamaras K and Tanner D B 1988 *Phys. Rev.* **B37** 1574
- Blumenroder S, Zirngiebl E, Schmidt H, Guntherodt G and Brenten H 1987 *Solid State Commun.* **64** 1229
- Hariharan Y, Janawadkar M P, Sastry V S and Radhakrishnan T S 1988 *Pramana - J. Phys.* **31** 1
- Hiroz Z, Takano M, Takeda Y, Kanno R and Bando Y 1988 *Jpn. J. Appl. Phys.* **27** L580
- Jayadev S, Rice M J and Wang Y R 1988 A model of the CuO₃ chain in the oxide superconductor Y₁Ba₂Cu₃O_{7-y}: electrons, excitons and charged phonons (Preprint)

- Kamaras K, Porter C D, Doss M G, Herr S L, Tanner D B, Bonn D A, Greedan J E, O'Reilly A H, Stager C V and Timusk T 1987 *Phys. Rev. Lett.* **59** 919
- Kirby P B, Harrison M R, Freeman W G, Samuel I and Haines M J 1987 *Phys. Rev.* **B36** 8315
- Kourouklis G A, Jayaraman A, Batlog B, Cava R J, Stavola M, Krol D M, Rietman E A and Schneemeyer L F 1987 *Phys. Rev.* **B36** 8320
- Maeno Y, Kato M, Aoki Y and Fujita T 1987 *Jpn. J. Appl. Phys.* **26** L1982
- Nasu S, Kitagawa H, Oda Y, Kohara T, Shinjo T, Asayama K and Fujita F E 1987 *Physica* **B148** 484
- Oda Y, Fujita H, Toyoda H, Kaneko T, Kohara T, Nakada I and Asayama K 1987 *Jpn. J. Appl. Phys.* **26** L1660
- Rice M J and Wang Y R 1987 *Phys. Rev.* **B36** 8794
- Roth G, Hegner G, Renker B, Pannetier J, Caignaert V, Hervieu M and Raveau B 1988 *Z. Phys.* **B** (Preprint)
- Ruani G, Tallani C, Zamboni R, Cittone D and Maticotta F C 1988 *Physica C* (Preprint)
- Saito Y, Sawada H, Iwazumi T, Abe Y, Ikeda H and Yoshizaki R 1987 *Solid State Commun.* **64** 1047
- Santoro A, Miraglia S, Beech F, Sunshine S A, Murphy D W, Schneemeyer L F and Waszczak J V 1987 *Mater. Res. Bull.* **22** 1007
- Sugai S 1987 *Phys. Rev.* **B36** 7133
- Takayama-Muromachi E, Uchida Y and Kato K 1987 *Jpn. J. Appl. Phys.* **26** L2087
- Thomsen C, Liu R, Bauer M, Wittlin A, Genzel L, Cardona M, Schonherr E, Bauhofer W and Konig W 1988a *Solid State Commun.* **65** 55
- Thomsen C, Cardona M, Kress W, Liu R, Genzel L, Bauer M and Schonherr E 1988b *Solid State Commun.* **65** 1139